Definition of the Representative Elementary Volume (REV) to elastic simulations in carbonate rocks from Morro do Chaves Formation – a Pre-Salt chronocorrelate.

André Martins*[1], Roseane Misságia[1], Herson Rocha[2], Marco Ceia[1], Jéssica Moreira[1], Lucas Oliveira[1], Sofia Bueno[1], Nathan Magalhães[1], [1] LENEP/UENF, [2] FACC.

Abstract

Digital rock physics (DRP) refers to a technique based on digital image analysis (DIA), which combines microtomography and other imaging techniques with advanced numerical simulations of effective material properties. The purpose of DRP is to determine, understand, and model the relationships between remotely-sensed geophysical observations and in-situ rock properties. By employing this approach, DRP offers a sophisticated means of characterizing complex petrophysical systems and predicting their behavior under various conditions. As with any other DIA method, DRP has the most critical step described in function of segmentation that must be as accurate as possible to guarantee fidelity in any further simulation. When processing the total sample size is not feasible defining a Representative Elementary Volume (REV) is an alternative. Given the necessity regarding the characterization of porous system and elastic behavior of rock samples, this paper applied a meticulous study of REV definition combined to a very careful selection of a thresholding method to segmentation step before a simulation of the elastic characteristics of a carbonate rock sample image. The results of pre-processing and REV study showed accuracy selecting a very representative region of the sample to be used in the characterization. Numerical simulations showed their importance to reservoir characterization, providing results that corroborates with laboratory measurements.

Introduction

Given the complexity of characterizing the geological properties of the Pre-Salt region, researchers aim to understand the origin of carbonate reservoirs including those containing coquinas. Outcrops are employed as analogs or chronocorrelate to facilitate plausible comparisons and extrapolations of this reservoir type. DIA has become an alternative tool to investigate the properties of materials and objects that are difficult to observe. DRP is a computational field that explores the physical and fluid flow properties of porous rocks within this context.

As with any other DIA method, DRP has the most critical step described in function of segmentation. This step of digital image analysis involves identifying different regions, faces, or objects of interest and ends when the objects or regions of interest have been detected (GONZALEZ and WOODS, 2008).

There are different automatic methods of segmentation that define threshold interval based on functions and equations, performing numerous iterations to guarantee accuracy in this step of image analysis (PREWITT and MENDELSOHN, 1966; OTSU, 1979; KAPUR, SAHOO, and WONG, 1985). Segmentation accuracy is critical for successful computational processing, requiring that investigated characteristics remain visible.

To represent the entire sample, defining a Representative Elementary Volume (REV) is an alternative when processing the total sample size is not feasible. The REV needs to be large enough to represent the sample's characteristics and as small as possible compared to its total volume (FERNANDES et al., 2012). The success of the REV definition determines the accuracy of estimating the reservoir properties.

In this context, given the necessity regarding the characterization of porous system and elastic behavior of rock samples, this paper aims to apply an accurate process of DRP in case to guarantee fidelity of the characteristics of the sample and perform a very rigorous REV study to provide a realistic elastic simulation of coquinas samples from Morro do Chaves Formation.

Methodology

Before performing any image simulation, there is a pre-processing that includes filters, brightness and contrast adjustment, and even smoothing to eliminate noise.

Different automatic thresholding methods were tested using IMAGE-J software to assure accuracy and fidelity in the segmentation process. In addition, for each method tested, the segmentation results were visualized in different image slices for quality checking.

The REV study includes cutting the total sample, according to Pereira (2018). This method consists of sample clippings in

- Partition in the three main orthogonal axes (X, Y, and Z), generating a total of 14 (fourteen) sub-volumes;
- Partition into fractions of ⅓, ⅔, ⅖, and ⅗ only for the X-axis, preserving the directions in the other main axes, directing in 14 (fourteen) sub-volumes.

This clipping method generates a total of 28 sub-volumes to be statistically evaluated using porosity as the

parameter to verify their similarities with the total sample (PEREIRA, 2018; VIK et al., 2013). The porosity of each sub-volume was statistically compared to the porosity of the entire sample to define REV.

Once the samples' REV is defined, the ElastoDict module of the GeoDict 2020 software is used to perform the numerical simulation of the elastic behavior of the sample.

The simulation employs a solver, FFT, which relies on the Fast Fourier Transform for voxel grid homogenization methods (Kabel et al., 2015), to compute the effective static elastic parameters (elastic tensor), furnish the local strains and stresses (comprising 3D views), and the complete stiffness tensor that is subsequently employed for anisotropy characterization. This approximation is used to determine elastic properties such as P- and S-wave velocities (Vp and Vs, respectively), Bulk (K), and Shear (G) moduli as follows (Shon, 2011).

$$Vp_{(V,H)} = \sqrt{\frac{C_{ij}}{\rho_{bulk}}} = \sqrt{\frac{M}{\rho_{bulk}}} = \sqrt{\frac{K+\frac{4}{3}G}{\rho_{bulk}}}, \quad (1)$$

$$Vs_{(V,H)} = \sqrt{\frac{C_{ij}}{\rho_{bulk}}} = \sqrt{\frac{G}{\rho_{bulk}}}, \quad (2)$$

$$\rho_{bulk} = (1-\phi)\rho_{min} + \rho_{fl}\phi\,. \quad (3)$$

were i and j index correspond to the line and column of the stiffness tensor matrix, ρ bulk is bulk density, ϕ is porosity, ρmin is the mineral density of rock frame, and ρfl is the density of pore fluid.

Subsequently, the estimated velocities are compared with those measured in the laboratory for validation purposes.

Figure 1 presents a flowchart of the methodology.

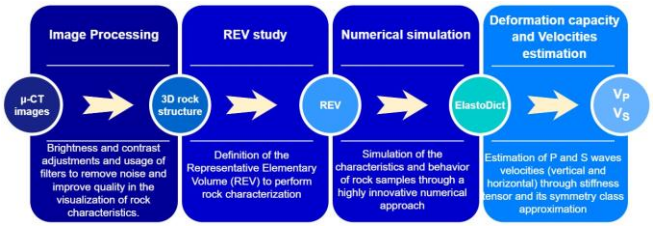

Figure 1- Methodology steps flowchart

Results and Discussions

Using IMAGE-J software, contrast and brightness adjustment and filter applications were made to highlight the characteristics of the image. In addition, different automatic thresholding methods were applied to μ-CT images of A18 and G32 samples to obtain accuracy in the segmentation step. Figures 2 and 3 present the results of pre-processing of the images and also the result of applying thresholding methods to segmentation.

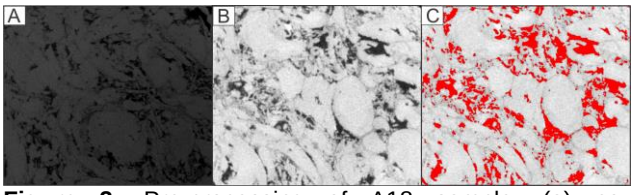

Figure 2- Pre-processing of A18 sample: (a) no treatment, (b) brightness and contrast adjustment and filter application, (c) result of segmentation (porosity in red).

Several thresholding methods use different mathematical approaches to identify the difference in intensity values of the gray levels. This allows the identification of the continuity and discontinuity in a part of the image. Applying and testing several thresholding methods available in IMAGE-J software, such as Renyi Entropy, Mean, Max Entropy, Otsu, Triangle, Minimum, Moments, and Intermodes. From all those, Intermodes and Otsu provided the best adjustments for samples A18 and G32, simultaneously.

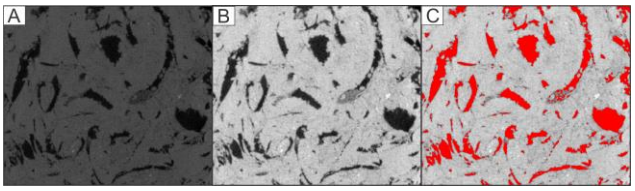

Figure 3- Pre-processing of G32 sample: (a) no treatment, (b) brightness and contrast adjustment and filter application, (c) result of segmentation (porosity in red).

The REV study was performed using porosity as a parameter for both samples A18 and G32. Figure 4 (A and B) present the statistical porosity analysis for the A18 and G32 sub-volume. The red point corresponds to the image with total volume (without crop), and the grey and orange points correspond to those sub-volumes larger than 500 mm^3. The yellow and blue points correspond to those sub-volumes smaller than 500 mm^3. There is a strong correlation between volume size, cropping region, and porosity, especially for sub-volumes with porosity greater than 10%, which have a polynomial correlation with R^2=0.98%. These sub-volumes show a better correlation between porosity and volume.

The sub-volumes smaller than 500 mm^3 (yellow and blue points) have expressed high instability in porosity values for the same size. There is a strong dependency on the crop region for such a small sub-volume.

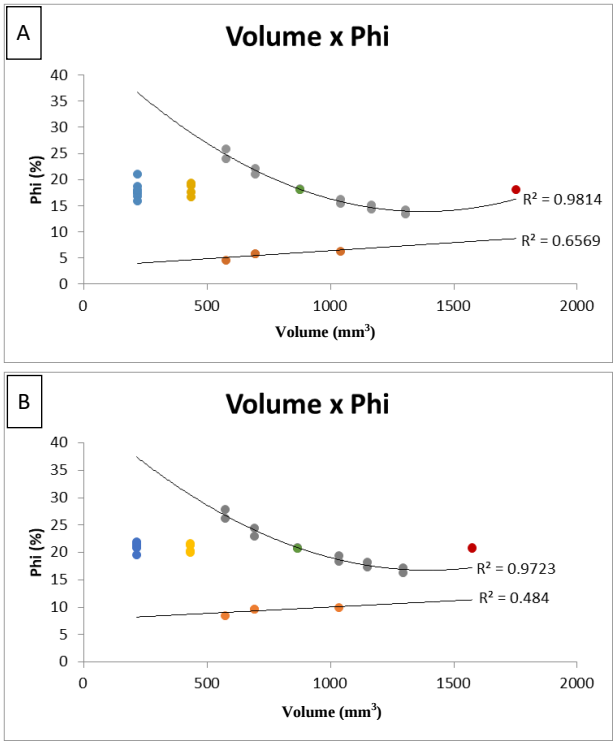

Figure 4- Porosity vs. Volume diagram for samples (a) A18 and (b) G32.

Green points are sub-volumes with the highest porosity correlation when compared to their original volumes, which we consider the best candidates for REVs. Elastic simulation in both REVs provides a symmetric anisotropy stiffness tensor for different symmetry classes and elastic/velocities purposes. Using the appropriated symmetry class stiffness tensor, the velocities were calculated. Table 1 presents the results of vertical and horizontal velocities for both, numerical simulation using the REVs and laboratory measurements in the rock samples.

Table 1- Compressional and shear horizontal and vertical velocities computed with the stiffness approximation tensor obtained with FFT numerical simulation for the coquina samples compared with ultrasonic measurements

Sample	Density (g/cm³)	Simulated parameters			
		V_{PH} (km/s)	V_{SH} (km/s)	V_{PV} (km/s)	V_{SV} (km/s)
A18	2.31	1.970	1.248	2.409	1.333
		Laboratory measured parameters			
		V_{PH} (km/s)	V_{SH} (km/s)	V_{PV} (km/s)	V_{SV} (km/s)
		2.54	1.495	2.593	1.601
G32	2.32	Simulated parameters			
		V_{PH} (km/s)	V_{SH} (km/s)	V_{PV} (km/s)	V_{SV} (km/s)
		2.427	1.461	2.877	1.331
		Laboratory measured parameters			
		V_{PH} (km/s)	V_{SH} (km/s)	V_{PV} (km/s)	V_{SV} (km/s)
		3.51	2.006	3.224	1.532

The sample G32 which has high porosity and low density presented higher values for vertical and horizontal velocities than the A18 sample, which expressed low porosity and high density.

Figures 5 and 6 show the simulated FFT polar plot and 3D visualization for strain for the three normal load directions (XX, YY, ZZ) obtained from 3D µ-CT coquinas samples.

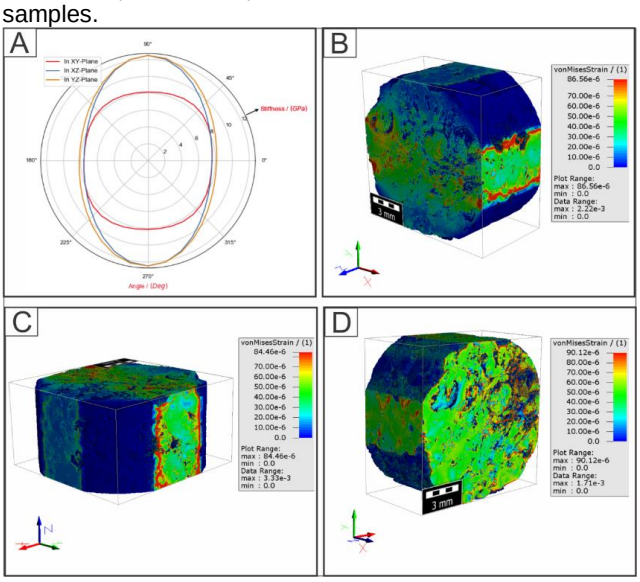

Figure 5- A18 simulated FFT: (a) polar plot of the direction-dependent stiffness in the XY, XZ, and YZ planes (anisotropic Young Modulus), (b) 3D visualization for strain in the YZ plane, (c) 3D visualization for strain in XZ plane.

Sample A18 presents a heterogeneous stiffness distribution. For both XZ and YZ, there are high stiffness values in 90° direction (approximately 12 GPa), but in the XY plane, the stiffness is about 8 GPa, expressing the most deformable plane. Based on this, 3D visualization presents regions of intermediate strain, with some high strain values on the Z-axis direction.

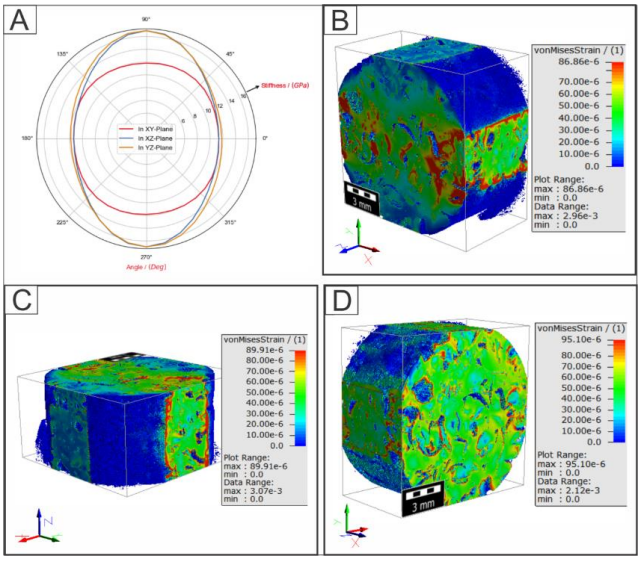

Figure 6- G32 simulated FFT: (a) polar plot of the direction-dependent stiffness in the XY, XZ, and YZ planes (anisotropic Young Modulus), (b) 3D visualization for strain in the YZ plane, (c) 3D visualization for strain in XZ plane.

Sample G32 presents similar stiffness behavior in XZ and YZ planes, with higher values in 90º. The XY plane, which corresponds to the Z-axis direction, presents lower stiffness. In concordance, the 3D deformation visualization expresses very low strain values, some close to zero. It is possible to see a region of high values of strain that may be associated with a preferential strain path in the Z-axis direction.

Conclusions

The pre-processing of images with filters and color adjustment was crucial and effective in improving the visualization of the sample characteristics.

The segmentation step depends on a good resolution and an excellent pre-processing step. Performing a study to define the best thresholding method to distinguish pore and matrix after appropriate treatments on the image ensured the quality of visualization of the characteristics, adding accuracy to the simulations.

The methodology for defining a Representative Elementary Volume (REV) accurately and effectively represents the sample petrophysical characteristics, improving accuracy and processing speed in numerical simulations. This is an essential consideration in digital image analysis once the definition of a representative volume can avoid over or underestimating the properties studied. However, refining the statistical analysis to guarantee precision and accuracy in the REV definition is essential. The methodology's numerical simulations provide accurate results, supporting laboratory measurements and expressing anisotropy. The uncertainties in the elastic simulation are related to the image resolution and the limitation of confinement pressure during laboratory measurements. It is known that the resolution can induce an under or overestimation of the petrophysical properties investigated (LIMA NETO et al., 2015).

These results highlight the importance of the high-resolution 3D image numerical simulation to improve understanding of the behavior and properties of rock samples. Notably, this consistent segmentation process improved pore and matrix identification, enhancing accuracy.

Acknowledgments

The authors thank UENF / LENEP for all environment and structure provided. We also thank ANP (Brazil's National Oil, Natural Gas, and Biofuels Agency) for the R&D levy regulation and for providing the rock samples. This study was financed in part by the CAPES/Brazil, PRH25-ANP/Finep, Equinor (Project No. 4600025270), CNPq, and INCT/Geofísica.

References

GONZALEZ, R.; WOODS, R. Digital Image Processing. New York: Pearson Prentice Hall, 2008.

J. N. KAPUR, P. K. SAHOO, and A. K. WONG, “A new method for gray level picture thresholding using the entropy of the histogram,” Computer vision, graphics, and image processing, vol. 29, no. 3, pp. 273–285, 1985.

J. PREWITT and M. L. MENDELSOHN, “The analysis of cell images,” Annals of the New York Academy of Sciences, vol. 128, no. 1, pp. 1035–1053, 1966.

KABEL M., MERKERT D, & SCHNEIDER M. (2015). Use of composite voxels in FFT-based homogenization. Computer Methods in Applied Mechanics and Engineering 294, 168-188.

LIMA NETO, I.A. Carbonate pore system evaluation under texture control for prediction of microporosity aspect ratio and shear wave velocity. Ph.D. thesis – Petroleum Reservoir & Exploration Engineering: North Fluminense State University (UENF) - Brazil-RJ, 2015.

OTSU, N. A Threshold Selection Method from Grey-level Histograms. [S.l.: s.n.], 1979.

PEREIRA, Felipe Pontual. ESTUDO ACERCA DO VOLUME ELEMENTAR REPRESENTATIVO EM AMOSTRAS DE COQUINAS ATRAVÉS DA PETROFÍSICA DIGITAL. 2018. Tese de Doutorado. Universidade Federal do Rio de Janeiro.

SCHNEIDER, C. A., RASBAND, W. S., & ELICEIRI, K. W. (2012). Nih image to IMAGEJ: 25 years of image analysis. Nature methods, 9(7), 671-675.

SCHÖN, J.H., 2011, Physical properties of rocks: Fundamentals and Principles of Petrophysics, Elsevier, Vol. 8.

VIK, B., BASTESEN, E., SKAUGE, A. “Evaluation of Representative Elementary Volume for a Vuggy Carbonate Rock – Part I: Porosity, Permeability, and Dispersivity”. In: Journal of Petroleum Science and Engineering, 112, pp. 36-47, 2013.